



## REVIEW

# Engineering Novel Molecular Beacon Constructs to Study Intracellular RNA Dynamics and Localization



Zhao Ma<sup>1,#,a</sup>, Xiaotian Wu<sup>1,#,b</sup>, Christopher J. Krueger<sup>1,2,c</sup>, Antony K. Chen<sup>1,\*,d</sup>

<sup>1</sup> Department of Biomedical Engineering, College of Engineering, Peking University, Beijing 100871, China

<sup>2</sup> Wallace H Coulter Department of Biomedical Engineering, Georgia Institute of Technology, Atlanta, GA 30332, USA

Received 8 January 2017; revised 8 April 2017; accepted 17 April 2017

Available online 21 September 2017

Handled by Akimitsu Okamoto

## KEYWORDS

2'-O-methyl RNA;  
Phosphorothioate;  
Molecular beacon;  
RNA dynamics;  
Single-molecule RNA  
imaging

**Abstract** With numerous advancements in novel biochemical techniques, our knowledge of the role of RNAs in the regulation of cellular physiology and pathology has grown significantly over the past several decades. Nevertheless, detailed information regarding RNA processing, trafficking, and localization in living cells has been lacking due to technical limitations in imaging single RNA transcripts in living cells with high spatial and temporal resolution. In this review, we discuss techniques that have shown great promise for single RNA imaging, followed by highlights in our recent work in the development of **molecular beacons** (MBs), a class of nanoscale oligonucleotide-probes, for detecting individual RNA transcripts in living cells. With further refinement of MB design and development of more sophisticated fluorescence microscopy techniques, we envision that MB-based approaches could promote new discoveries of RNA functions and activities.

RNA trafficking and localization are important processes that influence cellular physiology at the epigenetic, post-transcriptional, and post-translational levels. Conventional techniques such as qRT-PCR and DNA microarrays are cell lysate-based assays that provide ensemble averages of RNA expression levels. To improve our current understanding of the role of RNAs in health and disease, there is great interest among

RNA biologists to visualize individual RNAs in cells. There are currently three popular approaches — fluorescence *in situ* hybridization (FISH), the MS2 system, and molecular beacons (MBs) — commonly employed by researchers to study RNAs at the single-molecule level in various cellular contexts. Below, we discuss each technique's usage, advantages, and limitations.

## Single-molecule RNA imaging techniques

### Single-molecule FISH

Single-molecule FISH (smFISH) is a powerful technique that uses multiple fluorophores to visualize specific RNA targets

\* Corresponding author.

E-mail: [chenak@pku.edu.cn](mailto:chenak@pku.edu.cn) (Chen AK).

# Equal contribution.

<sup>a</sup> ORCID: 0000-0002-7635-8979.

<sup>b</sup> ORCID: 0000-0002-4655-4901.

<sup>c</sup> ORCID: 0000-0002-5070-9515.

<sup>d</sup> ORCID: 0000-0002-4105-9741.

at the single-molecule level in cells [1]. As detection of individual fluorophores by conventional fluorescence microscopy is difficult, in order to achieve single-molecule sensitivity, multiple fluorophore-tagged oligonucleotide probes are designed to target different regions of an RNA transcript [1–3]. Hybridization of multiple probes to the same RNA molecule renders the target RNA sufficiently fluorescent upon excitation, allowing each target transcript to be imaged as a bright spot (Figure 1A, Table 1). Currently, smFISH is regarded as the gold standard approach to visualize intracellular distributions of single RNA transcripts in fixed cells and tissues [1]. However, due to the required fixation steps, RNA dynamics data cannot be easily obtained using smFISH. Additionally, smFISH requires permeabilization to allow oligonucleotide probes to enter the cell and hybridize to the target RNAs and washing to remove unbound probes. Therefore, false-negative data can sometimes result from the loss of RNAs.

## MS2

The MS2 system takes advantage of the ability of the bacteriophage MS2 coat protein (MCP) to bind to an aptamer sequence (known as the MS2 aptamer) with high specificity and affinity (Figure 1B, Table 1) [4–7]. To enable single-RNA imaging, target RNA is genetically modified to harbor multiple tandem repeats of the MS2 aptamer. When co-expressed with an MCP-GFP fusion protein, each target RNA can then be tagged by multiple GFPs through MS2-MCP interactions, thus appearing as a bright fluorescent spot. To date, the MS2 system has been the most popular approach for imaging single engineered RNA transcripts in living cells, owing to its biostability and ease of delivery [4–8]. However, this approach cannot be used for imaging endogenous RNAs, and its use of fluorescent proteins limits fluorophore brightness that is necessary for high-quality imaging. Furthermore, MCP-GFP fusion proteins weigh nearly 40 kDa. Thus binding of multiple large probes to an RNA may potentially interfere with its normal activities and functions [9].

## MBs

MBs are antisense stem-loop forming oligonucleotide probes labeled with a fluorophore at one end and a quencher at the other end [10] (Figure 1C, Table 1). In the “closed” or “off” configuration, the complementary sequences flanking the loop domain anneal to form a stable stem, placing the quencher in close proximity with the reporter fluorophore, quenching its fluorescence. In the “open” or “on” configuration, target hybridization with the loop domain disrupts the stem, bringing the quencher away from the fluorophore to restore its fluorescence [10]. With careful selection of fluorophore-quencher pair, MB fluorescence can increase 20–100 fold upon hybridization to target RNA [11]. To date, MBs have been the most widely utilized tool for imaging endogenous RNA levels based on ensemble measurements [12–29]. To achieve single-molecule sensitivity, target RNA is engineered with tandem repeats of an MB target sequence, so that multiple MBs can hybridize to a target RNA, illuminating the RNA as a bright spot [30–32]. Despite these advantages, one major limitation for the use of MBs is their biostability. The chemistry of the MB oligonucleotide backbone influences susceptibility to nuclease degradation or non-specific protein binding, which could cause false-positive signals (FPSs) [14,19].

## Other potential techniques for single-molecule RNA imaging

In addition to the techniques described above, other techniques, including RNA-targeting CRISPR associated protein 9 (RCas9) [33], RNA-mimics of GFP-based systems [34], and sequence-specific Pumilio-based probes [35], have been developed for visualization of subcellular localization and trafficking of specific RNA molecules based on ensemble fluorescence measurement. Further work is required to explore their potential for imaging RNA transcripts in living cells at the single-molecule level.

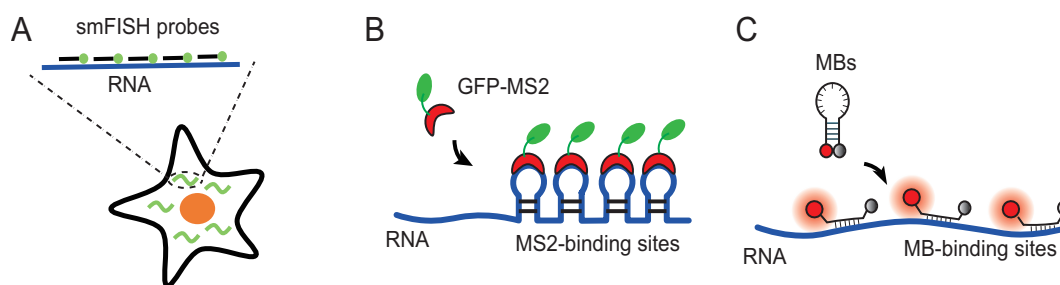


**Figure 1** Commonly-used techniques for single-molecule RNA imaging

**A.** smFISH labels an endogenous RNA molecule (blue line) in fixed cells using multiple oligonucleotide probes, with each probe designed to hybridize to a different region of the target RNA. **B.** The MS2 system requires engineering target RNA to harbor multiple MS2-binding sites (blue line) such that binding of GFP-MS2 fusion proteins (indicated in green and red, respectively) to the MS2-binding sites can cause the target RNA to appear as a bright fluorescent spot. **C.** MBs are stem-loop forming oligonucleotide probes that are labeled with a reporter (red circle) and a quencher (black circle). In the absence of MB target, the reporter is well-quenched. When hybridized to MB target, the fluorophore is separated from the quencher, resulting in restoration of fluorescence. When a target RNA is engineered to harbor multiple MB targets (blue line), hybridization of the MBs to MB targets can illuminate the engineered target RNA as a bright fluorescent spot. smFISH, single-molecule fluorescence in situ hybridization; MB, molecular beacon.

Table 1 Feature comparison of the currently-available approaches for single-molecule RNA imaging

Approach	Single molecule	Live-cell imaging	<i>In vivo</i> stability	Imaging endogenous RNAs	Probe size (kDa)	Fluorescent selection	High signal-to-background	Refs.
MB	Yes	Yes	Backbone chemistry dependent	Yes	~10	Organic fluorophore	Yes	[30–32]
MS2	Yes	Yes	YES	No	~40	Fluorescence protein	No	[4–8]
FISH	Yes	No	N/A	Yes	~10	Organic fluorophore	No	[1–3]

## MB attributes

Both the MS2 and MB systems are capable of imaging single RNA transcripts in living cells. Nonetheless, the MS2 system has been used more widely, despite the fact that MBs offer several advantages including smaller probe size, versatility in fluorophore/quencher selection, improved signal-to-background due to quenching, and the ability to image endogenous RNAs (Table 1). One major obstacle that hampers the widespread use of MBs is their tendency to be sequestered into the nucleus where they can generate FPSs as a result of nonspecific protein binding and/or nuclease degradation [14,19,20,22,31,36].

To reduce nonspecific signals, MBs have been conjugated to macromolecules that are either too big to traverse the nuclear pores, such as quantum dots [19] and pegylated NeutrAvidins [20], or are quickly exported to the cytoplasm, such as tRNAs [37] and small interfering RNA (siRNA)-like molecules [38]. Alternatively, MBs have been synthesized with degradation-resistant oligonucleotides containing locked nucleic acids (LNA) or modified internucleotide linkages (such as phosphorothioate, PS) [20,22,36]. By incorporating PS linkages throughout the loop domain of a 2'-O-methyl (2Me) MB backbone, we have recently developed an MB architecture called the 2Me/PS<sub>LOOP</sub> MB, based on the latter approach [31]. The 2Me/PS<sub>LOOP</sub> MB exhibits a marginal level of FPSs in various cell types and can be used for imaging single RNA transcripts in living cells [31]. Here we highlight the work undertaken to develop 2Me/PS<sub>LOOP</sub> MBs and explore their capabilities for single-molecule RNA imaging. We envision that the use of 2Me/PS<sub>LOOP</sub> MBs to study RNAs in living cells can further our knowledge of the role of RNAs in health and disease.

## Optimizing MB backbone chemistry for intracellular RNA analysis

Conventional MBs, including those that are synthesized with backbones composed of DNA or 2Me RNA linked with phosphodiester bonds (DNA or 2Me MBs), can be highly sensitive to nuclease degradation. To confer nuclease resistance, a non-bridging oxygen of the phosphate may be replaced with a sulfur atom to form a chemically-modified internucleotide linkage known as the PS bond. Yeh et al. reported the first use of MBs that incorporate PS linkages throughout the probe backbone (2Me/PS<sub>FULL</sub> MBs) and showed that these MBs enable detection of Coxsackie viral RNA replication for up to 12 h [20]. Supporting this finding, we showed that 2Me/PS<sub>FULL</sub> MBs have longer intracellular stability and bioactivity than 2Me MBs [36]. Despite these attributes, however, we found that 2Me/PS<sub>FULL</sub> MBs still cause a detectable FPS [36]. Several hours after entry, 2Me/PS<sub>FULL</sub> MBs could exhibit a punctate staining pattern that can be easily misinterpreted as RNA granules or even single RNA transcripts [31]. Puncta were primarily detected in the nucleus as expected, since highly-PS-modified oligodeoxyribonucleotides (ODNs) are widely reported to bind nonspecifically to the nuclear matrix [39–44].

We hypothesized that partially-PS-modified probes may exhibit an optimal balance of nuclease resistance while avoiding excess nonspecific binding. To test this, MBs were synthesized with different numbers and distributions of PS linkages. In a variety of cell types including HEK293, HeLa, Jurkat, and

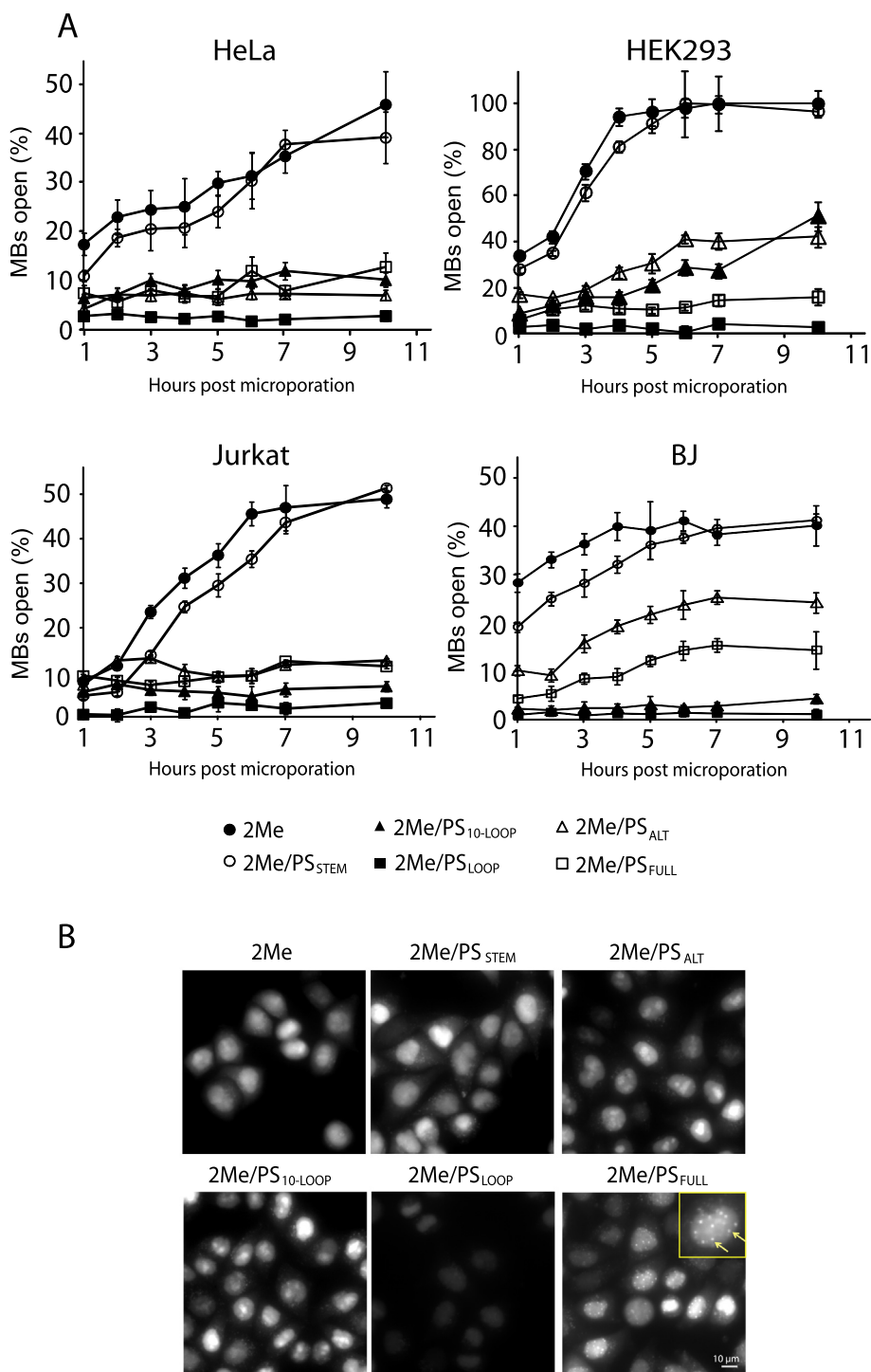


**Figure 2** Nonspecific opening of non-PS-modified and PS-modified MBs in living cells over time

Following microporation of 5 μM MBs that have no endogenous RNA targets into HeLa, HEK293, Jurkat, or primary BJ cells, the extent of MB opening was quantified over the course of 10 h [31]. The MBs tested include 2Me (●), 2Me/PS<sub>STEM</sub> (○), 2Me/PS<sub>10-LOOP</sub> (▲), 2Me/PS<sub>ALT</sub> (△), 2Me/PS<sub>LOOP</sub> (■), and 2Me/PS<sub>FULL</sub> (□). Data are presented as mean ± S.E. from at least 30 cells. **B**. Representative images of MBs in HeLa cells, acquired at 10 h post-microporation. The inset shows an expanded segment of the image. Arrows point to bright spots indicative of nonspecific binding in the nucleus (Scale bar, 10 μm). PS, phosphorothioate; MB, molecular beacon; 2Me, 2'-O-methyl. The graphs and images are reproduced with permission from Elsevier [31].

primary BJ cells, we observed a general trend of MB performance relative to the degree of PS modification (Figure 2). For example, 2Me MBs and 2Me/PS<sub>STEM</sub> MBs, which have

a fully PS-modified stem, were both highly susceptible to nonspecific opening [31]. Incorporating PS in the loop domain significantly improved MB stability, as 2Me/PS<sub>10-LOOP</sub> MBs

exhibited lower FPSs than 2Me/PS<sub>STEM</sub> MBs, despite having the same total number (10) of PS modifications. Consistent with this observation, 2Me/PS<sub>LOOP</sub> MBs, which have a fully-PS-modified loop domain and a phosphodiester stem, exhibited even lower FPSs than 2Me/PS<sub>10-LOOP</sub> MBs [31]. Only 1%–3% of the 2Me/PS<sub>LOOP</sub> MBs opened nonspecifically within 10 h after delivery into several different cell types [31]. FPSs generated by 2Me/PS<sub>LOOP</sub> MBs were lower than those generated by 2Me/PS<sub>FULL</sub> MBs, suggesting that when the loop domain is highly PS-modified, stem domain modification is disadvantageous, as the additional PS groups can induce nonspecific binding while offering no additional increase in nuclease resistance. Overall, these findings demonstrate the feasibility of reducing the number of PS modifications in the MB backbone to reduce nonspecific binding while maintaining nuclease resistance.

Currently, debate over the primary causes of MB FPSs in living cells remains unresolved. Our findings that MBs with different PS modifications exhibit large differences in the degree of nonspecific opening can help explain why MBs open nonspecifically in cells. For example, single-stranded endonucleases appear to be the primary cause of MB nonspecific opening, as levels of FPSs are inversely correlated with the extent of PS modifications in the single-stranded loop domain [31]. Exonucleases appear to have little impact on MB degradation, as PS modifications in the stem have little effect on MB stability [31]. Presumably, the fluorophore and the quencher sterically block access by 5'- and 3'-exonucleases. The tendency of highly-PS-modified MBs to aggregate and emit FPSs is consistent with previous studies showing that PS-modified ODNs are prone to nonspecific binding to cellular proteins [39–44]. Accordingly, the higher nonspecific signals emitted by 2Me/PS<sub>FULL</sub> than 2Me/PS<sub>LOOP</sub> MBs suggest that any nuclease resistance gained by PS modifications in the stem domain is offset by increased nonspecific binding due to greater number of PS modifications.

### Assessing the accuracy of 2Me/PS<sub>LOOP</sub> MBs for single-molecule RNA imaging

Our finding that 2Me/PS<sub>LOOP</sub> MBs exhibit a marginal level of FPS raises the possibility of using MBs to image the dynamics and localization of single RNA transcripts in living cells with high accuracy. To determine whether 2Me/PS<sub>LOOP</sub> MBs can accurately detect single RNA transcripts, we developed a plasmid construct that encodes a transcript carrying an EGFP coding sequence followed by 32 tandem repeats of an MB target sequence (pEGFP-N1-32x) [31]. As the MB target sequence and EGFP coding sequence are transcribed as one RNA molecule, we hypothesized that if MBs could hybridize to the engineered transcript, the target RNA should appear as a bright fluorescent spot reflecting MB-target hybridization. Furthermore, the MB fluorescent spot should colocalize with smFISH spots visualized using a set of probes targeting unique regions on the EGFP sequence. We found that following microporation of 2Me/PS<sub>LOOP</sub> MBs and smFISH processing, bright MB and smFISH spots could be detected in the nucleus and the cytoplasm (Figure 3A). Analysis of colocalization between MB and smFISH signals in three dimensions showed nearly 90% colocalization of the MB and smFISH signals, indicating that 2Me/PS<sub>LOOP</sub> MBs can detect engineered transcripts with

high accuracy (Figure 3B). By contrast, in cells microporated with 2Me/PS<sub>FULL</sub> MBs and processed by smFISH, only 60% of the MB signals colocalized with smFISH signals. Thus, consistent with the analysis showing that 2Me/PS<sub>LOOP</sub> MBs generate lower FPS compared to 2Me/PS<sub>FULL</sub> MBs, 2Me/PS<sub>LOOP</sub> MBs can image single RNA transcripts more accurately than 2Me/PS<sub>FULL</sub> MBs in living cells.

### Noninvasive imaging of RNA dynamics using 2Me/PS<sub>LOOP</sub> MBs

Given their ability to detect single engineered RNA transcripts with high accuracy in live cells, 2Me/PS<sub>LOOP</sub> MBs may be a promising tool to study the trafficking and localization of single RNA transcripts in real time. Figure 4A shows diffusion coefficients of single pEGFP-N1-32x RNAs in cells as measured by MB imaging. The high variance of diffusion coefficients among transcripts in both the nucleus and cytoplasm indicates a heterogeneous nature of RNA dynamics [31]. On average, RNAs in the nucleus move nearly 4 times slower than transcripts in the cytoplasm, consistent with previous findings showing that the nucleoplasm is more viscous than the cytoplasm [45]. Similar results have been obtained in cells transfected with pEGFP-C1-32x RNAs (Figure 4B), in which the 32 MB target repeats are located in the 3'-UTR. These findings suggest that an RNA transcript can be targeted by 2Me/PS<sub>LOOP</sub> MBs at either 5'- or 3'-UTR. Furthermore, binding of the 2Me/PS<sub>LOOP</sub> MBs to 32 tandem repeats does not cause interference with EGFP translation as seen when 64 repeats are used (Figure 4C), suggesting that MBs can be used to image target RNA containing up to 32 tandem repeats without perturbing physiological functions of target RNAs. There is no change in cell viability or cell spreading detected in cells microporated with varying concentrations of MBs (Figure 4D–E), suggesting that 2Me/PS<sub>LOOP</sub> MBs do not affect cellular growth or physiology. Overall, these findings suggest that 2Me/PS<sub>LOOP</sub> MBs can be a noninvasive platform for imaging single RNA transcripts in living cells.

### Conclusion

Conventional MBs have been used to image RNAs in various cellular contexts, but their propensity for nonspecific opening in living cells limits their widespread applications in studies where more sensitive detection is necessary, such as imaging RNA localization and dynamics at the single-molecule level [19,20,38]. We have recently developed a new MB architecture, known as the 2Me/PS<sub>LOOP</sub> MB, that elicits a marginal level of FPSs in cells as compared with conventional MBs [31]. We show that 2Me/PS<sub>LOOP</sub> MBs could accurately image single mRNA transcripts harboring 32 tandem repeats of an MB target sequence using conventional fluorescence microscopy. Currently, RNA dynamics at the single-molecule level has been studied primarily based on engineered RNA molecules that harbor large insertions of MB target or MS2 aptamer sites that potentially interfere with the activities of target RNAs. With further possible approaches for optimizing signal-to-background, such as fluorophore/quencher selection, and the use of more sophisticated imaging techniques, we anticipate that 2Me/PS<sub>LOOP</sub> MBs can be a promising platform for

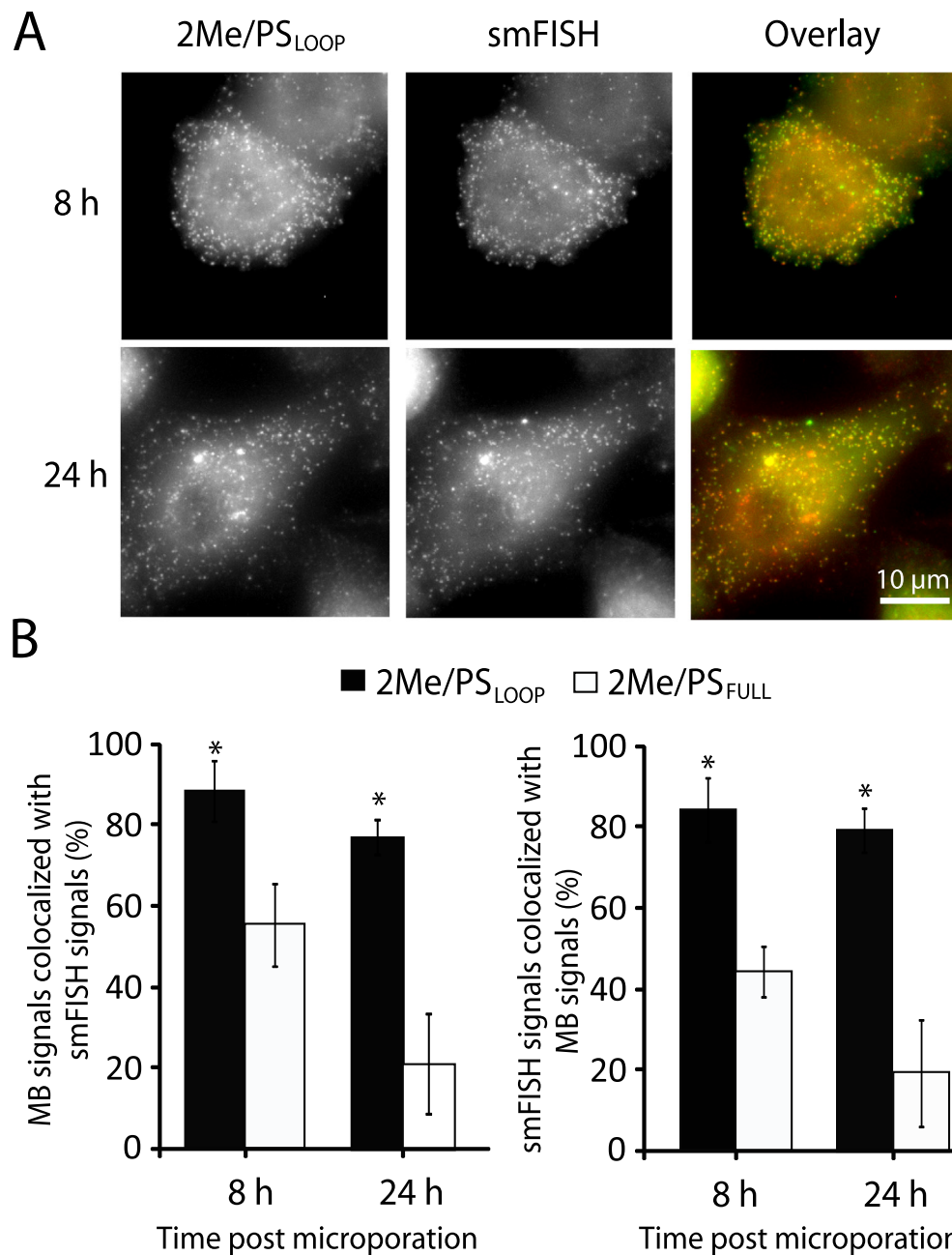


### Figure 3 Single-molecule RNA transcript detection using 2Me/PS<sub>LOOP</sub> MBs and smFISH

HeLa cells stably expressing pEGFP-N1-32x were fixed and permeabilized 8 h or 24 h after microporation with 5  $\mu$ M 2Me/PS<sub>LOOP</sub> MBs. smFISH was then performed with a pool of probes designed to target EGFP to assess MB detection accuracy for single RNA transcripts. **A.** Representative maximum intensity projection images of 2Me/PS<sub>LOOP</sub> MBs (Atto647NN-labeled) and EGFP smFISH probes (TAMRA-labeled) at 8 h or 24 h after microporation (Scale bar, 10  $\mu$ m). **B.** The percentage of MB signals that colocalized with smFISH signals (left) and the percentage of smFISH signals that colocalized with MB signals (right) was analyzed on a cell-by-cell basis using a custom MATLAB program. Data are presented as mean  $\pm$  SD from at least 10 cells. Significant difference from the 2Me/PS<sub>FULL</sub> MBs is indicated with asterisks ( $P < 0.05$ ). The images are reproduced with permission from Elsevier [31].

live-cell, single-molecule imaging of minimally-engineered RNA molecules, or even endogenous RNA molecules, providing researchers with opportunities to study RNAs with unprecedented spatial and temporal resolutions.

### Competing interests

The authors declare no conflict of interest.

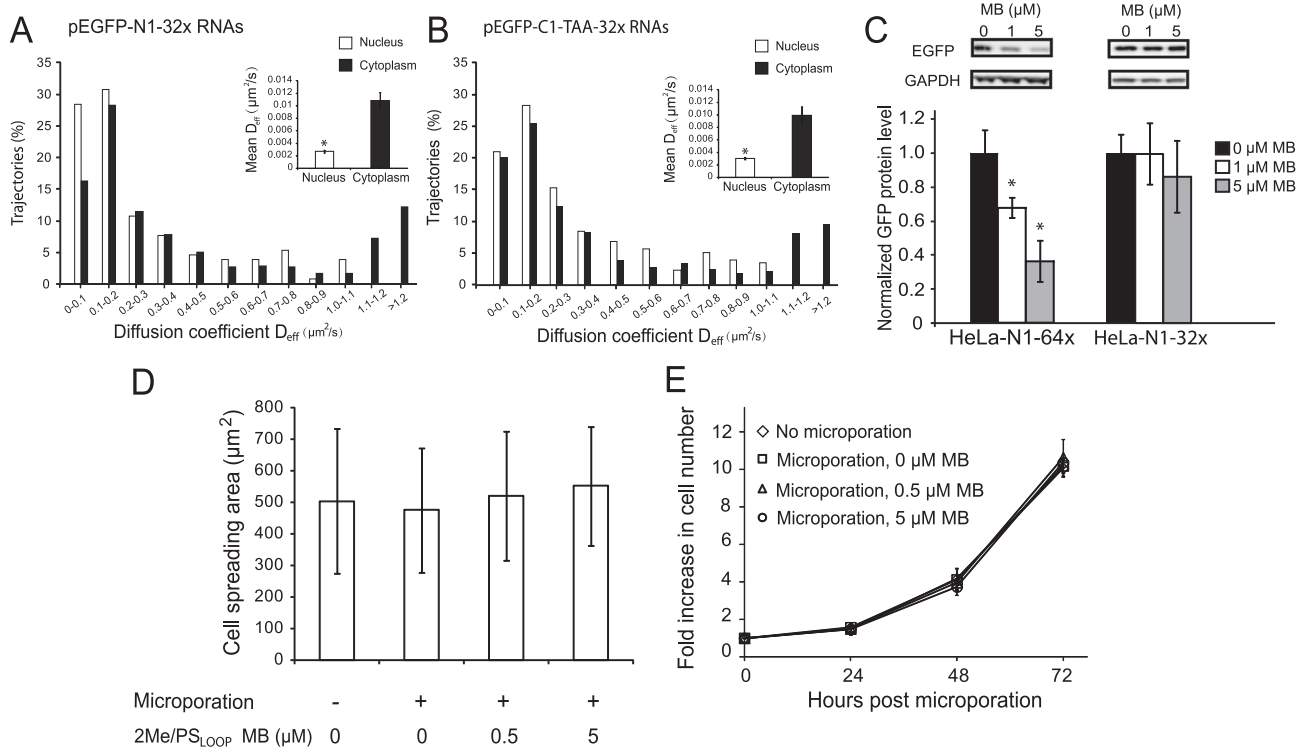


**Figure 4 Noninvasive imaging and measurement of RNA dynamics at the single-molecule level**

Single-particle tracking analysis reveals diffusion coefficients of single pEGFP-N1-32x (A) or pEGFP-C1-32x (B) mRNAs in the nucleus and the cytoplasm of HeLa cells. Insets show average diffusion coefficients (mean  $\pm$  SE) in the nucleus and the cytoplasm. Significant difference is indicated with asterisks ( $P < 0.05$ ). (C) The effect of 2Me/PS<sub>LOOP</sub> MBs on EGFP protein expression. Total EGFP protein level was assessed using Western blotting 24 h after microporation of 2Me/PS<sub>LOOP</sub> anti-repeat MBs at concentrations of 0, 1, or 5  $\mu\text{M}$  into HeLa cells stably expressing pEGFP-N1-32x or pEGFP-N1-64x RNAs. Protein expression is normalized to that in cells microporated with 0  $\mu\text{M}$  MB. Total GAPDH protein level was measured as a loading control. Significant difference from 0  $\mu\text{M}$  MBs is indicated with asterisks ( $P < 0.05$ ). Average spreading (D) and proliferation (E) 24 h after microporation with different concentrations of 2Me/PS<sub>LOOP</sub> MBs. All data are presented as mean  $\pm$  SD of at least three independent experiments. The images are reproduced with permission from Elsevier [31].

## Acknowledgments

This project was supported by grants from the National Key R&D Program of China (Grant Nos. 2016YFA0501603 and 2016YFA0100702), the National Natural Science Foundation of China (Grant Nos. 31771583 and 81371613), the Beijing Natural Science Foundation (Grant No. 7162114) and the 1000 Young Talent Program of China.

## References

- Raj A, van den Bogaard P, Rifkin SA, van Oudenaarden A, Tyagi S. Imaging individual mRNA molecules using multiple singly labeled probes. *Nat Methods* 2008;5:877–9.
- Chen F, Wassie AT, Cote AJ, Sinha A, Alon S, Asano S, et al. Nanoscale imaging of RNA with expansion microscopy. *Nat Methods* 2016;13:679–84.
- Tsanov N, Samacoits A, Chouaib R, Traboulsi AM, Gostan T, Weber C, et al. smiFISH and FISH-quant - a flexible single RNA detection approach with super-resolution capability. *Nucleic Acids Res* 2016;44:e165.
- Larson DR, Zenklusen D, Wu B, Chao JA, Singer RH. Real-time observation of transcription initiation and elongation on an endogenous yeast gene. *Science* 2011;332:475–8.
- Wu B, Chao JA, Singer RH. Fluorescence fluctuation spectroscopy enables quantitative imaging of single mRNAs in living cells. *Biophys J* 2012;102:2936–44.
- Ben-Ari Y, Brody Y, Kinor N, Mor A, Tsukamoto T, Spector DL, et al. The life of an mRNA in space and time. *J Cell Sci* 2010;123:1761–74.
- Katz ZB, English BP, Lionnet T, Yoon YJ, Monnier N, Ovrzyn B, et al. Mapping translation ‘hot-spots’ in live cells by tracking single molecules of mRNA and ribosomes. *Elife* 2016;5:e10415.
- Bertrand E, Chartrand P, Schaefer M, Shenoy SM, Singer RH, Long RM. Localization of *ASH1* mRNA particles in living yeast. *Mol Cell* 1998;2:437–45.
- Garcia JF, Parker R. MS2 coat proteins bound to yeast mRNAs block 5' to 3' degradation and trap mRNA decay products: implications for the localization of mRNAs by MS2-MCP system. *RNA* 2015;21:1393–5.
- Tyagi S, Kramer FR. Molecular beacons: probes that fluoresce upon hybridization. *Nat Biotechnol* 1996;14:303–8.
- Marras SA, Kramer FR, Tyagi S. Efficiencies of fluorescence resonance energy transfer and contact-mediated quenching in oligonucleotide probes. *Nucleic Acids Res* 2002;30:e122.

- [12] Bratu DP, Cha BJ, Mhlanga MM, Kramer FR, Tyagi S. Visualizing the distribution and transport of mRNAs in living cells. *Proc Natl Acad Sci U S A* 2003;100:13308–13.
- [13] Santangelo PJ, Nix B, Tsourkas A, Bao G. Dual FRET molecular beacons for mRNA detection in living cells. *Nucleic Acids Res* 2004;32:e57.
- [14] Tyagi S, Alsmadi O. Imaging native beta-actin mRNA in motile fibroblasts. *Biophys J* 2004;87:4153–62.
- [15] Drake TJ, Medley CD, Sen A, Rogers RJ, Tan W. Stochasticity of manganese superoxide dismutase mRNA expression in breast carcinoma cells by molecular beacon imaging. *Chembiochem* 2005;6:2041–7.
- [16] Kloc M, Wilk K, Vargas D, Shirato Y, Bilinski S, Etkin LD. Potential structural role of non-coding and coding RNAs in the organization of the cytoskeleton at the vegetal cortex of *Xenopus* oocytes. *Development* 2005;132:3445–57.
- [17] Wang A, Salazar AM, Yates MV, Mulchandani A, Chen W. Visualization and detection of infectious coxsackievirus replication using a combined cell culture-molecular beacon assay. *Appl Environ Microbiol* 2005;71:8397–401.
- [18] Santangelo P, Nitin N, LaConte L, Woolums A, Bao G. Live-cell characterization and analysis of a clinical isolate of bovine respiratory syncytial virus, using molecular beacons. *J Virol* 2006;80:682–8.
- [19] Chen AK, Behlke MA, Tsourkas A. Avoiding false-positive signals with nuclease-vulnerable molecular beacons in single living cells. *Nucleic Acids Res* 2007;35:e105.
- [20] Yeh HY, Yates MV, Mulchandani A, Chen W. Visualizing the dynamics of viral replication in living cells via Tat peptide delivery of nuclease-resistant molecular beacons. *Proc Natl Acad Sci U S A* 2008;105:17522–5.
- [21] Wang W, Cui ZQ, Han H, Zhang ZP, Wei HP, Zhou YF, et al. Imaging and characterizing influenza A virus mRNA transport in living cells. *Nucleic Acids Res* 2008;36:4913–28.
- [22] Wu Y, Yang CJ, Moroz LL, Tan W. Nucleic acid beacons for long-term real-time intracellular monitoring. *Anal Chem* 2008;80:3025–8.
- [23] Rhee WJ, Bao G. Simultaneous detection of mRNA and protein stem cell markers in live cells. *BMC Biotechnol* 2009;9:30.
- [24] Dong H, Ding L, Yan F, Ji H, Ju H. The use of polyethylenimine-grafted graphene nanoribbon for cellular delivery of locked nucleic acid modified molecular beacon for recognition of microRNA. *Biomaterials* 2011;32:3875–82.
- [25] Kang WJ, Cho YL, Chae JR, Lee JD, Choi KJ, Kim S. Molecular beacon-based bioimaging of multiple microRNAs during myogenesis. *Biomaterials* 2011;32:1915–22.
- [26] Yang L, Lin C, Liu W, Zhang J, Ohgi KA, Grinstein JD, et al. ncRNA- and Pc2 methylation-dependent gene relocation between nuclear structures mediates gene activation programs. *Cell* 2011;147:773–88.
- [27] Catrina IE, Marras SA, Bratu DP. Tiny molecular beacons: LNA/2'-O-methyl RNA chimeric probes for imaging dynamic mRNA processes in living cells. *ACS Chem Biol* 2012;7:1586–95.
- [28] Kim JK, Choi KJ, Lee M, Jo MH, Kim S. Molecular imaging of a cancer-targeting theragnostics probe using a nucleolin aptamer- and microRNA-221 molecular beacon-conjugated nanoparticle. *Biomaterials* 2012;33:207–17.
- [29] Jha R, Wile B, Wu Q, Morris AH, Maher KO, Wagner MB, et al. Molecular beacon-based detection and isolation of working-type cardiomyocytes derived from human pluripotent stem cells. *Biomaterials* 2015;50:176–85.
- [30] Vargas DY, Raj A, Marras SA, Kramer FR, Tyagi S. Mechanism of mRNA transport in the nucleus. *Proc Natl Acad Sci U S A* 2005;102:17008–13.
- [31] Zhao D, Yang Y, Qu N, Chen M, Ma Z, Krueger CJ, et al. Single-molecule detection and tracking of RNA transcripts in living cells using phosphorothioate-optimized 2'-O-methyl RNA molecular beacons. *Biomaterials* 2016;100:172–83.
- [32] Chen M, Ma Z, Wu X, Mao S, Yang Y, Tan J, et al. A molecular beacon-based approach for live-cell imaging of RNA transcripts with minimal target engineering at the single-molecule level. *Sci Rep* 2017;7:1550.
- [33] Nelles DA, Fang MY, O'Connell MR, Xu JL, Markmiller SJ, Doudna JA, et al. Programmable RNA tracking in live cells with CRISPR/Cas9. *Cell* 2016;165:488–96.
- [34] Paige JS, Wu KY, Jaffrey SR. RNA mimics of green fluorescent protein. *Science* 2011;333:642–6.
- [35] Ozawa T, Natori Y, Sato M, Umezawa Y. Imaging dynamics of endogenous mitochondrial RNA in single living cells. *Nat Methods* 2007;4:413–9.
- [36] Chen AK, Behlke MA, Tsourkas A. Sub-cellular trafficking and functionality of 2'-O-methyl and 2'-O-methyl-phosphorothioate molecular beacons. *Nucleic Acids Res* 2009;37:e149.
- [37] Mhlanga MM, Vargas DY, Fung CW, Kramer FR, Tyagi S. tRNA-linked molecular beacons for imaging mRNAs in the cytoplasm of living cells. *Nucleic Acids Res* 2005;33:1902–12.
- [38] Chen AK, Davydenko O, Behlke MA, Tsourkas A. Ratiometric bimolecular beacons for the sensitive detection of RNA in single living cells. *Nucleic Acids Res* 2010;38:e148.
- [39] Uhlmann E, Peyman A. Antisense oligonucleotides — a new therapeutic principle. *Chemical Reviews* 1990;90:543–84.
- [40] Stein CA, Cheng YC. Antisense oligonucleotides as therapeutic agents — is the bullet really magical? *Science* 1993;261:1004–12.
- [41] Brown DA, Kang SH, Gryaznov SM, DeDionisio L, Heidenreich O, Sullivan S, et al. Effect of phosphorothioate modification of oligodeoxynucleotides on specific protein binding. *J Biol Chem* 1994;269:26801–5.
- [42] Lorenz P, Baker BF, Bennett CF, Spector DL. Phosphorothioate antisense oligonucleotides induce the formation of nuclear bodies. *Mol Biol Cell* 1998;9:1007–23.
- [43] Weidner DA, Valdez BC, Henning D, Greenberg S, Busch H. Phosphorothioate oligonucleotides bind in a non sequence-specific manner to the nucleolar protein C23/nucleolin. *FEBS Lett* 1995;366:146–50.
- [44] Stein CA. Phosphorothioate antisense oligodeoxynucleotides: questions of specificity. *Trends Biotechnol* 1996;14:147–9.
- [45] Guilak F, Tedrow JR, Burgkart R. Viscoelastic properties of the cell nucleus. *Biochem Biophys Res Commun* 2000;269:781–6.